

Clickable 4-Oxo- β -lactam-Based Selective Probing for Human Neutrophil Elastase Related Proteomes

Eduardo F. P. Ruivo,^[a] Lídia M. Gonçalves,^[a] Luís A. R. Carvalho,^[a] Rita C. Guedes,^[a] Stefan Hofbauer,^[b, c] José A. Brito,^[b] Margarida Archer,^[b] Rui Moreira,^{*,[a]} and Susana D. Lucas^{*,[a]}

Human neutrophil elastase (HNE) is a serine protease associated with several inflammatory processes such as chronic obstructive pulmonary disease (COPD). The precise involvement of HNE in COPD and other inflammatory disease mechanisms has yet to be clarified. Herein we report a copper-catalyzed alkyne-azide 1,3-dipolar cycloaddition (CuAAC, or 'click' chemistry) approach based on the 4-oxo- β -lactam warhead that yielded potent HNE inhibitors containing a triazole moiety. The resulting structure-activity relationships set the basis to develop fluorescent and biotinylated activity-based probes as tools for molecular functional analysis. Attaching the tags to the 4-oxo- β -lactam scaffold did not affect HNE inhibitory activi-

ty, as revealed by the IC₅₀ values in the nanomolar range (56–118 nM) displayed by the probes. The nitrobenzoxadiazole (NBD)-based probe presented the best binding properties (ligand efficiency (LE)=0.31) combined with an excellent lipophilic ligand efficiency (LLE=4.7). Moreover, the probes showed adequate fluorescence properties, internalization in human neutrophils, and suitable detection of HNE in the presence of a large excess of cell lysate proteins. This allows the development of activity-based probes with promising applications in target validation and identification, as well as diagnostic tools.

Introduction

Serine hydrolases are one of the largest, most diverse and biologically important enzyme classes in eukaryotic and prokaryotic proteomes.^[1] Not surprisingly, an increasing number of clinically approved drugs target several members of this enzyme class such as lipases, esterases, amidases, and proteases. Human neutrophil elastase (HNE) is a member of the chymotrypsin family of serine proteases that degrades tissue matrix proteins such as elastin when released from the azurophilic granules in neutrophils due to inflammatory stimuli and mediators.^[2] Several pulmonary dysfunctions result from the massive migration of neutrophils to the lungs during inflammation and the subsequent release of proteolytic enzymes.^[2] The imbalance between HNE and its endogenous inhibitors leads to severe tissue injuries resulting in a variety of diseases

such as chronic obstructive pulmonary disease (COPD), rheumatoid arthritis, pulmonary emphysema, and psoriasis.^[3] Moreover, it has been postulated that HNE can contribute to the progression of non-small-cell lung cancer.^[4]

The need for understanding essential molecular recognition events in biological systems has directed considerable efforts toward the development of chemical probes.^[5] The design of small-molecule activity-based probes (ABPs) has proven to be a successful approach to track the spatial-temporal location and activity of proteases.^[6] Hence, the use of ABPs that target HNE may lead to an easy methodology for the quantification of HNE activity in lung disorders, and may ultimately lead to new diagnostic tools that function through non-invasive protocols.^[7,8]

The design of new HNE inhibitors has been intensively pursued, and exploiting the reactivity and molecular recognition properties of scaffolds used as enzyme inhibitors has led to breakthrough advances in the development of ABP warheads.^[6] G-quadruplex-based complexes were reported as the first efficient probes targeting HNE,^[9] but only recently have non-natural peptidic substrates of HNE been assembled as sensitive ABPs.^[7] This approach can be applied to HNE activity profiling as a promising tool to perform molecular function analyses of HNE-related disease proteomes. In addition, it has already been shown that the use of ABPs targeting HNE for the analysis of human specimens from patients with chronic lung diseases might lead to an efficient methodology for the validation of HNE as a diagnostic tool via a non-invasive protocol.^[10]

[a] E. F. P. Ruivo, Dr. L. M. Gonçalves, L. A. R. Carvalho, Dr. R. C. Guedes, Prof. R. Moreira, Dr. S. D. Lucas
Research Institute for Medicines (iMed.Ulisboa), Faculty of Pharmacy, Universidade de Lisboa, Av. Prof. Gama Pinto, 1649-003 Lisbon (Portugal)
E-mail: sdlucas@ff.ulisboa.pt
rmoreira@ff.ulisboa.pt

[b] Dr. S. Hofbauer, Dr. J. A. Brito, Dr. M. Archer
Instituto de Tecnologia Química e Biológica—António Xavier, Universidade Nova de Lisboa, Avenida da República, 2780-157 Oeiras (Portugal)

[c] Dr. S. Hofbauer
Present address: Department for Structural and Computational Biology, Max F. Perutz Laboratories, University of Vienna, 1030 Vienna (Austria)

Supporting information and the ORCID identification number(s) for the author(s) of this article can be found under <http://dx.doi.org/10.1002/cmdc.201600258>.

Kasperkiewicz et al.^[7] reported non-natural peptidic substrates of HNE as sensitive ABPs, revealing that the level of active HNE during the process of neutrophil extracellular trap formation was not as high as anticipated, highlighting the utility of this approach in dissecting biological events. As the use of peptidic substrates can raise some challenges, herein we present the use of small-molecular scaffolds as ABPs that provide both ease of handling and high specificity toward the target protein. A 1,2,3-triazole-based oxo- β -lactam library was synthesized to rapidly explore the impact of the triazole moiety on HNE inhibitory potency. This information was then extended to the design of ABPs that were validated for HNE activity. Neutrophil internalization and selectivity in the presence of a complex proteome was observed for an ABP containing a nitrobenzoxadiazole (NBD) tag. Moreover, a bio-orthogonal probing methodology is envisaged, as the starting oxo- β -lactam alkyne was also shown to inhibit HNE.

Results and Discussion

1,2,3-Triazole-based 4-oxo- β -lactams are potent HNE inhibitors

Previous 4-oxo- β -lactam structure–activity relationship (SAR) studies against HNE showed that diethyl substitution at C3 is preferred for optimal S_1 subsite recognition, leading to improved inhibitory activity and target selectivity. Furthermore, the N-substitution pattern can be explored as an anchor to probe the interaction with S_n subsites (Figure 1).^[11,12]

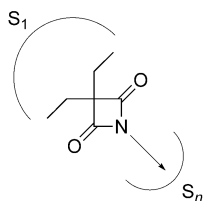


Figure 1. Schematic representation of the spatial arrangement of oxo- β -lactam substituents in the active site of HNE.

Click chemistry is as a powerful and versatile synthetic tool for drug development and chemical biology applications.^[13,14] More specifically, copper-catalyzed alkyne–azide 1,3-dipolar cycloaddition (CuAAC) has been explored as an efficient approach for the generation of compound libraries,

where the formed 1,2,3-triazole moiety is more than a passive linker, as it presents favorable physicochemical properties.^[15] We first prepared the 4-oxo- β -lactam alkyne **1** (Table 1) as the starting material for CuAAC chemistry. Remarkably, compound **1** showed to be a potent inhibitor of HNE, with an IC_{50} value of 82 nM (Table 1), while displaying a fragment-like nature [$M_r = 179.22$ Da, ligand efficiency (LE) = 0.81, lipophilic ligand efficiency (LLE) = 5.53].^[16,17]

With this encouraging result in hand, we then synthesized a small set of 1,2,3-triazole-based 4-oxo- β -lactam derivatives, **2a–I** (Table 1) by reacting alkyne **1** with the appropriate azides. Compounds **2a–I** revealed to be very potent HNE inhibitors, with IC_{50} values ranging from 14 to 103 nM (Table 1). These values compare favorably with that determined for ONO-5046 (15 nM), the only HNE inhibitor in clinical use and included as a positive control in our assay. Although there was some loss

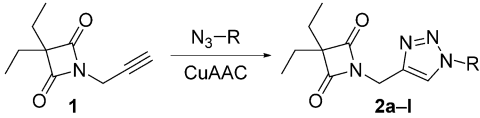
of LE as result of fragment growth, all compounds **2** displayed LE values >0.3 , thus meeting the requirements of an early lead. Furthermore, LLE values remained in the range of 5–6, reflecting the fact that lipophilicity was kept fairly constant during fragment growth, and suggesting that the 1,2,3-triazole moiety may lead to additional interactions with the enzyme active site.

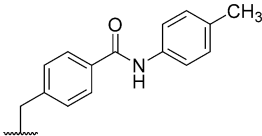
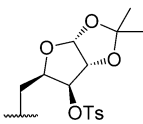
To gain molecular insight on the preferred interactions of the synthesized compounds and the active site of HNE, molecular docking studies were performed using HNE coordinates from PDB ID: 3Q77.^[18] All the compounds showed a correct pose for the oxo- β -lactam in the S_1 pocket, promoting Ser195 nucleophilic attack in agreement with high activities obtained for the synthesized library (further details and molecular poses are given in the Supporting Information). We were unable to co-crystallize a triazole-based oxo- β -lactam either with HNE or porcine pancreatic elastase (PPE), but we have crystallized^[19] and determined the X-ray structure of PPE in complex with the closely related diethyl *N*-(methyl)pyridinyl-substituted oxo- β -lactam, at 1.8 Å resolution (Figure 2A, details of structure determination are given in the Supporting Information, and the atomic coordinates and structure factor amplitudes have been deposited in the RCSB Protein Data Bank (PDB) as PDB ID: 4YM9). This structure confirmed the expected covalent mechanism of action, involving ring opening and the suitable accommodation of the diethyl moiety in the S_1 pocket. Additional π – π stacking with His57 is likely to contribute to the stability of the complex, decreasing the rate of hydrolysis and promoting strong inhibition.

Design and synthesis of oxo- β -lactam-based probes

The encouraging results obtained with 1,2,3-triazole-substituted 4-oxo- β -lactams as HNE inhibitors led us to design a group of ABPs in which NBD, fluorescein, and biotin moieties were used as reporter tags and attached to the 4-oxo- β -lactam warhead via a 1,2,3-triazole linker (**3–5**, Figure 3). Docking studies revealed that the tag did not affect the positioning of the oxo- β -lactam ring inside the active site of HNE when compared with smaller triazole analogues (Figure S2, Supporting Information). Moreover, covalent docking performed using the coordinates from the PPE–oxo- β -lactam complex showed that the acyl-enzyme formed after Ser195 attack presents additional π – π stacking between the triazole moiety and His57 and cation– π stacking with the PPE backbone Arg61 residue (Figure 2B, ABP **3** example), that may increase the complex lifetime toward feasible ABP profiling.

The synthetic strategy was first to bind a tag moiety with a linker containing an appropriate handle for further reaction with the oxo- β -lactam alkyne **1** using CuAAC, yielding the NBD-, fluorescein-, and biotin-tagged probes **3–5** (Figure 3). To validate compounds **3–5** as potential ABPs, their activity was measured against HNE, showing conserved inhibitory activity as anticipated, with remarkable IC_{50} values in the nanomolar range (56–118 nM), deeming the structures as potent HNE inhibitors and suitable candidates for an ABP. The NBD-based probe **3** displayed the best binding properties (LE =

Table 1. Oxo- β -lactams synthesized by Huisgen 1,3-dipolar cycloaddition.


Compd	R	Yield [%]	IC ₅₀ [nM] ^[a]	LE [kcal mol ⁻¹]	LLE
1	-	21	82 ± 15	0.81	5.53
2a	Ph	18	21 ± 6	0.50	5.63
2b	C ₆ H ₄ -4-Me	25	18 ± 3	0.48	5.34
2c	C ₆ H ₄ -4-CF ₃	28	48 ± 1	0.40	4.36
2d	C ₆ H ₄ -4-OMe	41	19 ± 9	0.46	5.71
2e	C ₆ H ₄ -4-Br	35	25 ± 7	0.47	4.82
2f	CH ₂ Ph	62	103 ± 10	0.44	4.78
2g	CH ₂ C ₆ H ₄ -4-NO ₂	47	14 ± 4	0.43	5.94
2h	CH ₂ C ₆ H ₄ -4-Cl	74	17 ± 1	0.46	5.01
2i	CH ₂ C ₆ H ₄ -4-OMe	31	20 ± 5	0.44	5.41
2j	C ₆ H ₄ -2-NO ₂	58	31 ± 6	0.41	5.62
2k		44	16 ± 6	0.33	4.68
2l		94	30 ± 5	0.28	4.91
ONO-5046	-	-	15 ± 1	-	-

[a] Against HNE; values are the mean ± SD of *n* = 3 experiments performed in triplicate.

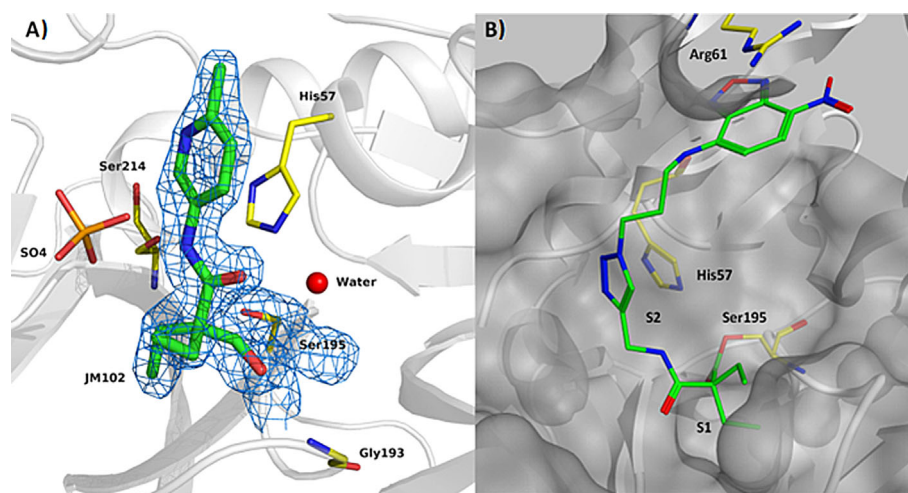


Figure 2. A) View of the active site of PPE complexed with a diethyl *N*-(methyl)pyridinyl-substituted oxo- β -lactam (JM102, PDB ID: 4YM9). The simulated annealing omit map is shown as a blue mesh contouring JM102; surrounding residues are shown in stick format: O: red, N: blue, S: gold, C: yellow (protein) and green (inhibitor). B) Covalent docking of compound 3 using the coordinates of the PPE-oxo- β -lactam complex (PDB ID: 4YM9).

0.31) combined with excellent lipophilic ligand efficiency (LLE = 4.7).

ABP 3 was characterized for its spectroscopic properties in solvents with various polarities. It was observed that the absorption and fluorescence of ABP 3 did not change with solvents of different polarities, which indicates that these probes

can be used for a variety of assays under different conditions (Figure S4).

Fluorescent ABPs 3 and 4 were incubated for 30 min with human neutrophils in order to test neutrophil internalization, where HNE is localized in biological systems. By comparing ABPs 3 and 4 (Figure 4A) with the DAPI-stained nuclei (Fig-

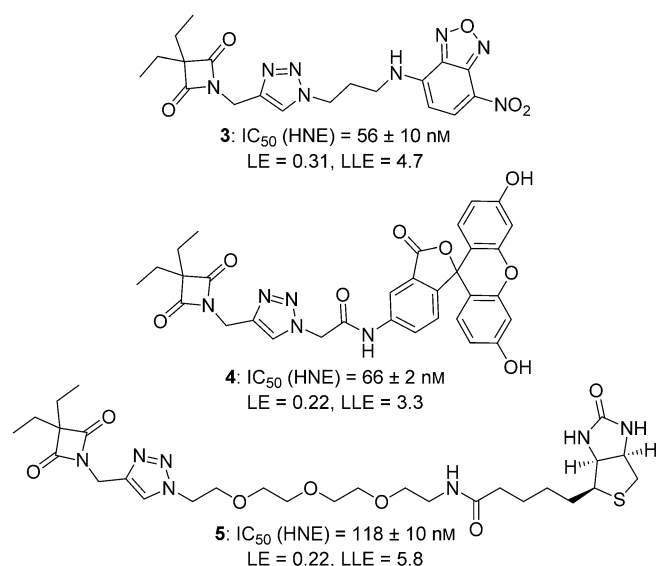


Figure 3. Oxo- β -lactam-based probes **3–5**.

ure 4B), it was observed that these were co-localized with the stained nuclei, indicating that both NBD- and fluorescein-tagged ABPs **3** and **4** were internalized in the neutrophils (Figure 4C).

The capacity of **3** and **4** to be internalized by neutrophils highlights the advantages of our small-warhead-based ABPs over the less permeable peptidic probes and expands the scope of biological assays that can be performed, allowing HNE visualization not only in neutrophil extracellular traps, but also in its intracellular localization. Moreover, the nanomolar biotinylated ABP will allow quantification and identification of targets by affinity isolation.

Selectivity for HNE was evaluated for the most potent inhibitor **2g**, ABP **3**, and the oxo- β -lactam containing the alkyne handle **1** against five related proteases (Table 2). Inhibitor **2g** (IC_{50} HNE = 14 nM) showed outstanding selectivity for HNE over

Table 2. Enzyme selectivity assay.			
Enzyme	IC_{50} [μ M] ^[a]		
	1	2g	3
HNE	0.082	0.014	0.056
PR3	8 ± 1	> 100	3 ± 1
Chymotrypsin	> 100	> 100	23 ± 1
Urokinase	> 100	> 100	12 ± 1
Trypsin	> 100	> 100	> 100
Thrombin	ND ^[b]	41 ± 2	1 ± 1

[a] Values are the mean \pm SD of $n=3$ experiments performed in triplicate.
[b] Not determined.

related proteases, displaying selectivity indices (SI) of > 2900. The oxo- β -lactam alkyne **1** exhibited a good selectivity profile, with SI > 100 toward all proteases studied, thus being a good candidate for bioorthogonal chemistry. The ABP **3** (IC_{50} HNE = 56 nM) was able to maintain an excellent selectivity profile, a remarkable achievement usually observed only with peptidomimetic probes.^[7,20] Overall, the results show suitable HNE selectivity for activity-based protein profiling.

Moreover, depending on the target proteomes, further assays are needed to evaluate experimental specificity. Hence, ABPs **3** and **4** were applied to label HNE in the presence of a complex proteome (HEK293T cell line was chosen as being a non-carcinogenic human cell line that does not express elastase) and subjected to SDS-PAGE for analysis by protein staining and fluorescence imaging (Figure 5). Remarkably, this assay revealed selective labelling of HNE in the presence of a large excess of lysate proteins without nonspecific interactions of either NBD or fluorescein ABPs **3** and **4**. SDS-PAGE showed unique HNE-ABP fluorescent bands (lanes 8 and 9, Figure 5B) clearly detected at the HNE region (for HNE control, lane 5, Figure 5), that was not observed in the absence of HNE (lanes 3 and 4, Figure 5B), revealing good selectivity of the fluorescent oxo- β -lactam ABPs for HNE.

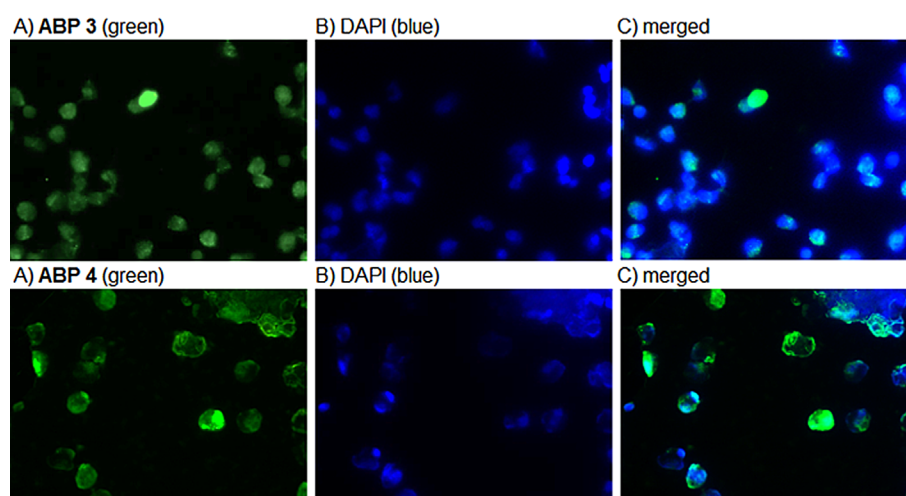


Figure 4. A) Human neutrophils after 30 min contact with ABPs **3** (top row) and **4** (bottom row). B) Nuclei stained with DAPI, incubation with ABP. C) Merged images.

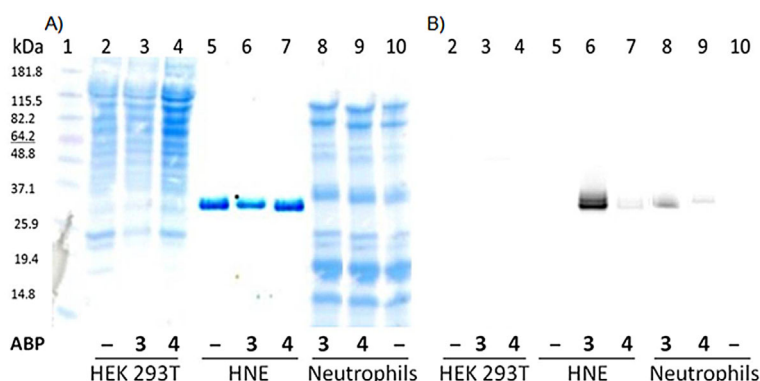


Figure 5. Imaging human leukocyte elastase with the fluorescent probes ABP 3 and 4 by SDS-PAGE. Laser image scanned at excitation wavelength 532 nm and 580 nm bandpass emission filter (Typhoon Trio) before total protein staining (B) and SDS-PAGE Coomassie blue labeling (A). Lanes 1: pre-stained protein standard markers, 2: 5 μg HEK293T protein extracts, 3: 5 μg HEK293T protein extracts and 1 μM ABP 4, 4: 5 μg HEK293T protein extracts and 1 μM ABP 3, 5: 40 ng HNE and 1 μM ABP 4, 7: 40 ng HNE and 1 μM ABP 3, 8: 5 μg human neutrophil protein extracts and 1 μM ABP 4, 9: 5 μg human neutrophil protein extracts and 1 μM ABP 3, 10: 5 μg human neutrophil protein extracts.

The amount of HNE for labeling experiments was decreased down to 5 ng (lanes 2–4, Figure 6), and a clear band was observed for ABP 3 detection in each lane, which strongly supports the suitability of the synthesized probes for low-nanogram-level detection of HNE.

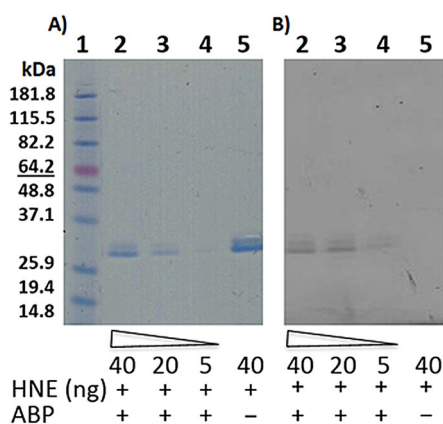


Figure 6. Imaging human leukocyte elastase with the fluorescent probe ABP 3 by SDS-PAGE. Laser image scanned at excitation wavelength 532 nm and 580 nm bandpass emission filter (Typhoon Trio) before total protein staining (B) and SDS-PAGE Coomassie blue labeling (A). Lanes 1: pre-stained protein standard markers, 2: 40 ng HNE and 1 μM ABP 3, 3: 20 ng HNE and 1 μM ABP 3, 4: 5 ng HNE and 1 μM ABP 3, 5: 40 ng HNE.

Conclusions

From the results presented in this work, we can conclude that clickable 4-oxo- β -lactams give access to potent and selective inhibitors against HNE and are valuable scaffolds for emerging molecular profiling approaches. The click chemistry approach proved to be an efficient tool for the development of new potent HNE inhibitors in which the 1,2,3-triazole moiety provides additional interactions in the enzyme active site. Proof-of-concept was performed with NBD-, fluorescein-, and biotin-tagged ABPs 3–5 that show conservation of the potent inhibi-

tory activity against HNE together with adequate fluorescence properties, internalization in human neutrophils, and suitable detection of HNE in the presence of a large excess of cell lysate proteins. The biotinylated probe is envisaged for further affinity isolation and quantification of HNE in inflammation-related proteomes. Moreover, a bio-orthogonal probing methodology can be foreseen by the use of the oxo- β -lactam alkyne 1 that may help to overcome possible cell permeability pitfalls. Notably, 1 exhibited a remarkable IC_{50} value of 82 nM (Table 1), a result consistent with the observation that the HNE inhibitory potency of 4-oxo- β -lactams is determined largely by the intrinsic reactivity of the 4-oxo- β -lactam warhead combined with the diethyl group at C3, responsible for molecular recognition. The ABPs presented herein will be further studied as promising tools for molecular mechanism studies of HNE-related diseases, namely COPD. Taken together, the results presented in this work highlight not only the versatility of the oxo- β -lactam scaffold for the generation of protease inhibitor libraries, but also the possibility to develop ABPs with promising applications in target validation and identification as well as in the development of diagnostic tools.

Experimental Section

3,3-Diethyl-1-(prop-2-yn-1-yl)azetidione-2,4-dione (1): To a stirring solution of diethylmalonyl dichloride (36 mmol, 6.3 mL) in dry dioxane (21 mL) at room temperature under nitrogen atmosphere, a solution of propargylamine (1 equiv, 2.3 mL) in the same solvent (21 mL) was added dropwise. A solution of triethylamine (18 mL) in dry dioxane (21 mL) was then also added dropwise, and the reaction was stirred at room temperature overnight. The solid residues were filtered and washed with hexanes. The filtered solution was concentrated, and the resulting residue was purified by flash chromatography, using a gradient of hexanes/EtOAc (0–100% EtOAc) to yield the desired alkyne 1 as a colorless waxy solid (1.35 g, 21%). ^1H NMR (400 MHz, CDCl_3): δ = 4.07 (d, J = 1.6 Hz, 2H), 2.31 (s, 1H), 1.76 (q, J = 7.5 Hz, 4H), 1.00 ppm (t, J = 7.5 Hz, 6H).

Synthesis of azide building blocks: Azide building blocks were synthesized from the corresponding bromides, chlorides, or tri-

fluoromethanesulfonates by reaction with sodium azide and used without further purification. For the azide precursor of compound **2j**, a synthetic procedure via diazonium salt using 2-nitroaniline as starting material was used. Further details are given in the Supporting Information.

Copper-catalyzed alkyne–azide 1,3-dipolar cycloaddition; Typical example for the synthesis of ABP 3: To a 0.1 M solution of alkyne **1** (0.32 mmol, 57 mg) in DMF, *N*-(3-azidopropyl)-7-nitrobenzoxadiazol-4-amine (1.1 equiv, 91.8 mg), aqueous sodium ascorbate (0.1 M, 10% mmol) and aqueous copper sulfate (0.1 M, 10% mmol) were added. The reaction was stirred overnight, and the reaction mixture was diluted with water (four volumes) and then extracted with EtOAc (3×1 volume). The organic layers were combined, dried with anhydrous Na₂SO₄, filtered and concentrated. The obtained residue was purified by flash chromatography (elution with hexanes/EtOAc gradient) followed by recrystallization from CH₂Cl₂/*n*-hexane to yield the target compound as an orange solid (94.5 mg, 67%); mp: 199–201 °C; ¹H NMR (300 MHz, (CD₃)₂SO): δ = 9.59 (brs, 1H), 8.56 (d, *J* = 8.9 Hz, 1H), 8.21 (s, 1H), 6.39 (d, *J* = 8.8 Hz, 1H), 4.63 (s, 2H), 4.56 (t, *J* = 6.9 Hz, 2H), 3.30 (m, 2H), 2.29 (quint, 2H), 1.72 (q, *J* = 7.5 Hz, 4H), 0.91 ppm (t, *J* = 7.5 Hz, 6H); ESIMS(+) *m/z*: 443 [*M* + H]⁺; Anal. calcd (C₁₉H₂₂N₈O₅): C 51.58, H 5.01, N 25.33%, found: C 51.79, H 5.21, N 25.34%.

In vitro enzyme activity assays: Enzymatic activities of oxo-β-lactam triazole derivatives were measured by conventional methods. The detailed procedures are given in the Supporting Information. All tested compounds had a purity of ≥ 95% as determined by elemental analysis.

X-ray analysis: Crystals of porcine pancreatic elastase (PPE) in complex with a diethyl *N*-(methyl)pyridinyl-substituted oxo-β-lactam inhibitor JM102 (PDB ID: 4YM9^[19]) were grown by using the vapor-diffusion hanging-drop method, and data were collected in an X8 Proteum X-ray diffractometer coupled with a Platinum¹³⁵-CCD detector at 100 K. Further details are given in the Supporting Information.

Molecular docking: The 3D structure coordinates of HNE were obtained from the Protein Data Bank (PDB ID: 3Q77) with X-ray coordinates at 2.00 Å resolution; for PPE: PDB ID: 4YM9 coordinates were used at 1.85 Å resolution. To prepare the enzymes for docking studies, Molecular Operating Environment (MOE) 2013.10 software package tools were used, and docking studies were then performed with the GoldScore scoring function from the GOLD software package as previously described.^[21] Further details are given in the Supporting Information.

Acknowledgements

This work was funded by Fundação para a Ciência e a Tecnologia (FCT, Portugal): PTDC/BBB-BEP/2463/2014, Pest-OE/SAU/UI4013/2014, PTDC/BIA-PRO/118535/2010, PEst-OE/EQB/LA0004/2011, SFRH/BPD/79224/2011 (J.A.B.), SFRH/BD/100400/2014 (L.A.R.C.), and IF/00472/2014 (S.D.L.). E.F.P.R. acknowledges a research grant awarded by Fundação AstraZeneca Innovate Competition (Portugal). iNOVA4Health Research Unit (LISBOA-01-0145-FEDER-007344), which is co-funded by FCT/MCES through national funds and by FEDER under PT2020, is acknowledged. The authors

thank Dr. Maria Elisa Alves for neutrophil collection and isolation from healthy donor samples, Prof. Isabel Sá-Correia (IST-ULisboa) for access to the Multimager system Thyphon Trio 6300583, Dr. Miguel Pessanha and Dr. Przemyslaw Nogly for help with X-ray structure characterization, and Dr. Paula Gomes for MS data acquisition at Faculdade de Ciências da Universidade do Porto.

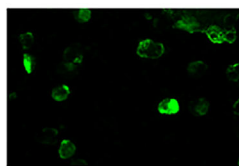
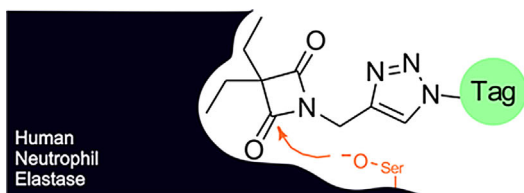
Keywords: 4-oxo-β-lactams • activity-based probes • click chemistry • fluorescent probes • human neutrophil elastase

- [1] D. A. Bachovchin, B. F. Cravatt, *Nat. Rev. Drug Discovery* **2012**, *11*, 52–68.
- [2] B. Korkmaz, M. S. Horwitz, D. E. Jenne, F. Gauthier, *Pharmacol. Rev.* **2010**, *62*, 726–759.
- [3] S. D. Lucas, E. Costa, R. C. Guedes, R. Moreira, *Med. Res. Rev.* **2013**, *33*, E73–E101.
- [4] G. Moroy, A. J. P. Alix, J. Sapi, W. Hornebeck, E. Bourguet, *Anti-Cancer Agents Med. Chem.* **2012**, *12*, 565–579.
- [5] M. Vendrell, D. T. Zhai, J. C. Er, Y. T. Chang, *Chem. Rev.* **2012**, *112*, 4391–4420.
- [6] a) T. Böttcher, S. A. Sieber, *MedChemComm* **2012**, *3*, 408–417; b) L. E. Sanman, M. Bogyo, *Annu. Rev. Biochem.* **2014**, *83*, 249–273; c) L. I. Willems, H. S. Overkleeft, S. I. van Kasteren, *Bioconjugate Chem.* **2014**, *25*, 1181–1191; d) L. Carvalho, E. Ruivo, S. D. Lucas, R. Moreira, *MedChemComm* **2015**, *6*, 536–546.
- [7] P. Kasperkiewicz, M. Poreba, S. J. Snipas, H. Parker, C. C. Winterbourn, G. S. Salvesen, M. Drag, *Proc. Natl. Acad. Sci. USA* **2014**, *111*, 2518–2523.
- [8] E. Deu, M. Verdoes, M. Bogyo, *Nat. Struct. Mol. Biol.* **2012**, *19*, 9–16.
- [9] K. H. Leung, H. Z. He, V. P. Y. Ma, H. Yang, D. S. H. Chan, C. H. Leung, D. L. Ma, *RSC Adv.* **2013**, *3*, 1656–1659.
- [10] G. Paone, V. Conti, A. Vestri, A. Leone, G. Puglisi, F. Benassi, G. Brunetti, G. Schmid, I. Cammarella, C. Terzano, *Dis. Markers* **2011**, *31*, 91–100.
- [11] J. Mulchande, R. C. Guedes, W. Y. Tsang, M. I. Page, R. Moreira, J. Iley, *J. Med. Chem.* **2008**, *51*, 1783–1790.
- [12] J. Mulchande, R. Oliveira, M. Carrasco, L. Gouveia, R. C. Guedes, J. Iley, R. Moreira, *J. Med. Chem.* **2010**, *53*, 241–253.
- [13] H. C. Kolb, M. G. Finn, K. B. Sharpless, *Angew. Chem. Int. Ed.* **2001**, *40*, 2004–2021; *Angew. Chem.* **2001**, *113*, 2056–2075.
- [14] P. Thirumurugan, D. Matosiuk, K. Jozwiak, *Chem. Rev.* **2013**, *113*, 4905–4979.
- [15] J. L. Hou, X. F. Liu, J. Shen, G. L. Zhao, P. G. Wang, *Expert Opin. Drug Discovery* **2012**, *7*, 489–501.
- [16] C. W. Murray, D. A. Erlanson, A. L. Hopkins, G. M. Keseru, P. D. Leeson, D. C. Rees, C. H. Reynolds, N. J. Richmond, *ACS Med. Chem. Lett.* **2014**, *5*, 616–618.
- [17] A. L. Hopkins, G. M. Keseru, P. D. Leeson, D. C. Rees, C. H. Reynolds, *Nat. Rev. Drug Discovery* **2014**, *13*, 105–121.
- [18] a) S. D. Lucas, L. M. Goncalves, L. A. R. Carvalho, H. F. Correia, E. M. R. Da Costa, R. A. Guedes, R. Moreira, R. C. Guedes, *J. Med. Chem.* **2013**, *56*, 9802–9806; b) G. Hansen, H. Gielen-Haertwig, P. Reinemer, D. Schomburg, A. Harrenga, K. Niefind, *J. Mol. Biol.* **2011**, *409*, 681–691.
- [19] S. Hofbauer, J. A. Brito, J. Mulchande, P. Nogly, M. Pessanha, R. Moreira, M. Archer, *Acta Crystallogr. Sect. F* **2015**, *71*, 1346–1351.
- [20] a) B. C. Lechtenberg, P. Kasperkiewicz, H. Robinson, M. Drag, S. J. Riedl, *ACS Chem. Biol.* **2015**, *10*, 945–951; b) R. Grzywa, E. Burchacka, M. Lecka, L. Winiarski, M. Walczak, A. Lupicka-Slowik, M. Wysocka, T. Burster, K. Bobrek, K. Csencsits-Smith, A. Lesner, M. Siencyzyk, *ChemBioChem* **2014**, *15*, 2605–2612.
- [21] GOLD ver. 5.1: <https://www.ccdc.cam.ac.uk/solutions/csd-discovery/components/gold/> (accessed July 19, 2016).

Received: May 19, 2016

Revised: June 28, 2016

Published online on ■ ■ ■ ■ 0000



E. F. P. Ruivo, L. M. Gonçalves, L. A. R. Carvalho, R. C. Guedes, S. Hofbauer, J. A. Brito, M. Archer, R. Moreira, S. D. Lucas**



Clickable 4-Oxo- β -lactam-Based Selective Probing for Human Neutrophil Elastase Related Proteomes



Click here! Human neutrophil elastase (HNE) is a serine protease implicated in several inflammatory processes. A click chemistry approach is reported based on the 4-oxo- β -lactam warhead toward the development of fluorescent and

biotinylated activity-based probes as tools for molecular functional analysis. The proof-of-concept study revealed selective detection of HNE activity in human neutrophils and in the presence of a large excess of cell lysate proteins.